

Quasiparticle excitations and ballistic transport in the mixed state of mesoscopic superconductors

A. S. Mel'nikov^{1,2} and V. M. Vinokur²

¹*Institute for Physics of Microstructures, Russian Academy of Sciences, 603950, Nizhny Novgorod, GSP-105, Russia*

²*Argonne National Laboratory, Argonne, Illinois 60439*

(Received 4 January 2002; published 5 June 2002)

As the size of the superconducting sample with a few fluxoids is less than the dephasing length new physics comes into play. The quasiparticle excitations in vortices form coherent quantum-mechanical states providing thus a possibility to control the phase-coherent transport through the sample by changing the number of fluxoids and their configuration. Thus, mesoscopic samples with a few vortices realize a new type of magnetically tunable Andreev waveguides. The sample conductance measured in the direction of the applied magnetic field is determined by the transparency of different multivortex configurations (giant multiquanta vortices and vortex molecules) which form a set of quantum channels. The transmission coefficient for each channel is controlled by multiple Andreev reflections within the vortex cores and at the sample edge. These interference processes result in a stepwise and/or oscillating behavior of the conductance as a function of the applied magnetic field. This is a vortex-based switch with the magnetic field playing the role of the gate voltage.

DOI: 10.1103/PhysRevB.65.224514

PACS number(s): 74.25.Ha, 74.60.Ec

Modern microfabrication techniques opened a route for studies of small superconducting structures of the size of several coherence lengths. The pioneering works^{1,2} revealed a rich variety of different phases within given fluxoid states. Magnetic field can penetrate the sample in the form of a polygonlike vortex molecule or individual vortices can merge forming multiquanta giant vortex. This transformation occurs via the second-order phase transition. First-order izomeric transitions between the different configurations of vortex molecule seen as branching of the magnetization curves can also take place. Numerical Ginzburg-Landau calculations (see, e.g., Ref. 3) confirmed that indeed vortices either merge into a single giant vortex with a certain winding number m or arrange in stable molecularlike configurations⁴ with vortex spacing a . The appealing question now is what are the resulting electronic states associated with different fluxoid structures and how do structural transitions in the vortex state of a mesoscopic superconductor affect its electronic properties. The low lying quasiparticle (QP) states bound at the isolated vortex core carrying the flux quantum $\phi_0 = \pi\hbar c/e$ were found first by Caroli, de Gennes, and Matricon⁵ and can be viewed as the formation of standing quasiparticle waves due to Andreev reflection of quasiparticles from the superconducting gap profile $\Delta(\vec{r})$ confining the vortex core. The quantitative theory of the quasiparticle states is based on the Bogolubov-de Gennes (BdG) equations, and in s superconductors the QP spectrum for small values of the angular momentum quantum number μ is $\varepsilon_\mu = \mu\Delta/(k_r\xi)$, where Δ is the gap value far from the vortex axis, ξ is the coherence length, $k_r = |\vec{k}_\perp|$, \vec{k}_\perp is the wave vector in the plane perpendicular to the vortex, and μ is half an odd integer. This is the so-called *anomalous branch* of the QP energy, which, as function of μ , varies from $-\Delta$ to Δ crossing zero as the impact parameter $b = \mu/|\vec{k}_\perp|$ of the particle in the core varies from $-\infty$ to $+\infty$.

In this paper we report our findings on peculiarities of the electronic structure of the QP Andreev states in a few-fluxoid superconductor (FFS). We also analyze the phase-coherent

transport through these states and demonstrate that conductance due to Andreev states in FFS's reveals a variety of oscillating behaviors. In particular, we find that local ballistic conductance can alternate between the finite and the near-zero values as a function of magnetic field. In this regime the mesoscopic superconductor thus realizes a quantum vortex switch where the external magnetic field plays the role of gate voltage.⁶

The bound states in the core can barely feel the presence of the neighboring vortices as long as the intervortex distance a is much larger than the coherence length ξ , i.e., as long as $H \ll H_{c2}(a \gg \xi)$. The formation of multiquanta vortices in infinite samples is not energetically favorable, which can be understood as a result of the strong repulsion forces between the singly quantized vortices. On the contrary, in small enough mesoscopic samples multiquanta structures may become stable for $H < H_{c2}$ due to compression forces from shielding Meissner currents pushing vortices to the center of the sample. As the distances between vortices compare to the coherence length $a \leq \xi$, wave functions overlap, interference effects come into play, and fundamentally new features of the QP spectrum, controlled by the geometry of both the vortex molecule and the sample, appear as a result of confinement. In small samples with radius R comparable to the coherence length the behavior of the vortex states will also be strongly affected by the edge electronic states. The finite magnetic field suppresses order parameter near the disk edge creating a potential well for quasiparticles. Bound quasiparticle states form due to both normal quasiparticle reflection at the disk edge and Andreev reflection from the boundary of the classically unpenetratable region. The local density of states (DOS) in such mesoscopic disc (measured, e.g., by the STM technique) should exhibit strong oscillations as a function of magnetic field. At the disk edge the period of these oscillations (with an increase in magnetic field) should correspond to the flux quantum, while at the disk center one can observe two-quanta periodic behavior (which is caused, in fact, by the Aharonov-Bohm effect).

The distinctive features of the electronic states in a multivortex configuration stem from their underlying mechanism, the multiple Andreev reflections from superconducting—normal-metal boundaries which are formed in an applied magnetic field. The phase-coherent quasiparticle transport in the direction perpendicular to the disk plane should be strongly influenced by this Andreev interference pattern. It was Giaever first who in his classic work⁷ noticed that when magnetic flux gets trapped in the superconductor, the small normal areas in parallel with superconducting areas appear that influence transport characteristics. We find that phase-coherent transport carried by the quasiparticle Andreev states associated with these normal domains realizes another of Giaever's visions:⁷ "Finally I would like to propose a different tunneling experiment: an experiment to determine if it is possible to tunnel through a superconductor. If so we have an ideal triode, because I can change the tunneling probability by changing the biasing potential of the superconductor." We focus here on another possibility to control this tunneling probability by changing the number of vortex lines in a mesoscopic sample. A quasiparticle incident upon the sample with a trapped vortex can propagate along the flux line provided its energy coincides with a certain energy level in the core. Otherwise, if this resonance condition is not fulfilled the wave function appears to decay along the vortex line at a certain decay length L_d . The ratio of this length to the sample thickness L determines the single-particle tunneling probability through the sample. The conducting channels with $L_d > L$ are open for single-particle tunneling, while the transport through the channels with $L_d \leq L$ is possible only because of two-particle Andreev processes. Because of the suppression of the order parameter in the vortex core the maximum decay length L_d appears to be much larger than the coherence length ξ (in the absence of vortices $L_d < \xi$). Changing the number and configuration of vortices we can control the transparency of the sample with respect to single-particle tunneling.

I. QUANTUM MECHANICS OF QUASIPARTICLES IN A FEW-FLUXOID DISK

The magnetic field induced low-energy branches in the quasiparticle spectrum appear due to: (i) decrease in the energy threshold for QP's binding to the sample edge, caused by both the suppression of the superconducting order parameter near the edge in a strong field and by the Doppler shift of the quasiparticle energy (such a mechanism results in formation of the surface bound states^{8,9}) and (ii) vortex penetration into the sample and, thus, formation of normal vortex-core regions confining quasiparticles.

A. The model

The quantum mechanics of quasiparticles is governed by the Bogolubov–de Gennes theory [We do not consider here ultrasmall samples (see, e.g., Ref. 10 and references therein) having a quantum level spacing $\delta\varepsilon$ comparable with the bulk superconducting gap. So in our case $\delta\varepsilon \ll \Delta$ the conventional (mean field) theory of superconductivity can be applied.]. In a conventional s-wave superconductor BdG equations are

$$\hat{h}_0 \left(-i\nabla + \frac{\pi}{\phi_0} \vec{A} \right) u(\vec{r}) + \Delta(\vec{r})v(\vec{r}) = \varepsilon u(\vec{r}), \quad (1)$$

$$-\hat{h}_0 \left(i\nabla + \frac{\pi}{\phi_0} \vec{A} \right) v(\vec{r}) + \Delta^*(\vec{r})u(\vec{r}) = \varepsilon v(\vec{r}), \quad (2)$$

where (u, v) are the particlelike and holelike parts of the QP wave function and Δ (energy gap) is the order parameter used in the Ginzburg-Landau (GL) theory. The corresponding one-particle Hamiltonian \hat{h}_0 in the most simple isotropic case takes the form

$$\hat{h}_0(\vec{k}) = \hbar^2 \vec{k}^2 / (2M) - E_F,$$

where E_F is the Fermi energy and M is the electron effective mass.

For simplicity and also in order to relate to the most common experimental situation, we consider a thin disk of the thickness $d < \lambda$ (λ is the London penetration depth) and radius $R \ll \lambda_{\text{eff}} = \lambda^2/d$. We use a cylindrical coordinate system (r, θ, z) with the z axis chosen perpendicular to the disk and origin at the disk center. The boundary conditions at the edge of the disk are $u(R, \theta) = 0, v(R, \theta) = 0$. In order to describe vortex molecules of general symmetry the order parameter can be conveniently written in the form

$$\Delta = \Delta_0 [\Psi(r) e^{im\theta} + D(r)],$$

where Ψ is a general solution of the GL equations for a multiquanta vortex located at the disk center in an external magnetic field H . The asymptotical behavior of the Ψ function at small distances $r \ll r_c$ (where r_c is the core radius) from the disk center is given by the expression $\Psi \sim (r/r_c)^m$. Near the disk edge the order parameter Ψ is also suppressed by the supercurrents. The function D is used to describe the splitting of a giant multiquanta vortex into individual vortices which are situated at a certain distance a from the disk center. This function is assumed to decay exponentially with an increase of distance r at a certain length scale $r_d \sim r_c$. Thus, for a small size of a vortex molecule ($a \ll r_c$) $D(0) \propto (a/r_c)^m$. It can be shown that for $D(r) = 0$ the QP angular momentum is conserved and the eigenfunctions $\hat{\varphi} = (u, v)$ can be written in the form⁵

$$\hat{\varphi}_\mu = \exp(ik_z z + i\mu\theta + i\hat{\sigma}_z m\theta/2) \hat{f}_\mu(r), \quad (3)$$

where the $\hat{f}_\mu(r)$ function is determined from the following set of equations:

$$\begin{aligned} \hat{\sigma}_z \frac{\hbar^2}{2M} \left[-\hat{f}_{rr} - \frac{1}{r} \hat{f}'_r + \left(\frac{\mu}{r} + \hat{\sigma}_z \frac{M}{\hbar} V_s(r) \right)^2 \hat{f} - k_r^2 \hat{f} \right] + \hat{\sigma}_x \Delta \hat{f} \\ = \varepsilon \hat{f}. \end{aligned} \quad (4)$$

The orbital momentum quantum number μ is an integer for even m , and half an odd integer for odd m values. Here $\hat{\sigma}_x, \hat{\sigma}_y, \hat{\sigma}_z$ are Pauli matrices, $k_r^2 + k_z^2 = k_F^2$, and

$$V_s = \frac{\hbar}{2M} \left(\frac{m}{r} + \frac{2\pi}{\phi_0} A_\theta \right)$$

is a superfluid velocity. For small disks of the radius $R \ll \lambda_{\text{eff}}$ we can neglect the screening effects and the vector potential can be taken in the form $A_\theta = -Hr/2$.

B. Edge bound states

We start with the analysis of the spectrum of QP's bound to the disk edge. The surface bound states appear due to the formation of a potential well caused by normal reflection at the surface and Andreev reflection at magnetic field induced spatial variations of the order parameter and superfluid velocity.^{8,9} To obtain the spectrum as a function of the angular momentum and magnetic field we follow the standard quasiclassical procedure described, for instance, in Ref. 9 and take the solution in the form

$$\hat{f}_\mu = \hat{A} e^{iS} + \text{c.c.}$$

Far from the vortex cores the quasiclassical approximation appears to be justified since both the superfluid velocity V_s and the GL order parameter $\Psi \approx \sqrt{1 - 4M^2 \xi^2 V_s^2 / \hbar^2}$ change on a length scale which is much larger than the coherence length ξ . For fields close to the field of the first vortex entry ($H \sim H^* = \phi_0 / \pi R \xi$) the supercurrent density results in a rather strong suppression of the order parameter absolute value as well as in a rather large Doppler shift (of the order of the gap value) of the energy of states with large impact parameters. As a consequence, the low-energy excitations appear to be localized near the disk edge. The spectrum of the states bound to the disk edge can be found using the Bohr-Sommerfeld quantization rule

$$\int_{\rho_t}^1 (P_+ - P_-) d\rho = \pi(n + \gamma). \quad (5)$$

Here $\rho = r/R$, n is an integer, γ is a quasiclassical constant of the order of unity, ρ_t is a coordinate of the turning point, and the momenta $P_\pm = R(S'_r)_\pm$ that are found from BdG equations have the form

$$\begin{aligned} \frac{P_\pm^2}{k_F^2 R^2} &= q^2 \left(1 - \frac{\tilde{b}^2}{\rho^2} \right) \pm \frac{2}{k_F \xi} \\ &\times \sqrt{\left[E + \frac{q\tilde{b}}{2\rho} \left(\frac{\rho H}{H^*} - \frac{m\xi}{\rho R} \right) \right]^2 + \left(\frac{\rho H}{H^*} - \frac{m\xi}{\rho R} \right)^2} - 1, \end{aligned} \quad (6)$$

where $q = k_r/k_F$, $E = \varepsilon/\Delta_0$, and $\tilde{b} = \mu/(k_r R)$ is a dimensionless impact parameter and μ is an orbital momentum quantum number. Bound quasiparticle states form due to both normal quasiparticle reflection at the disk edge and Andreev reflection from the boundary $r = r_t = \rho_t R$ of the classically unpenetrable region (see Fig. 1). To the lowest order in ξ/R the turning point ρ_t is determined by the expression

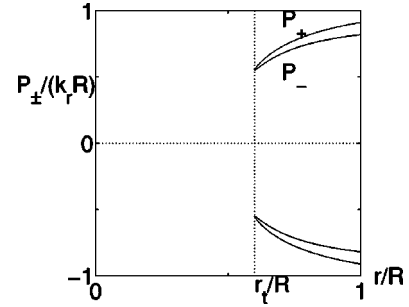


FIG. 1. Normalized quasiclassical radial momentum P vs distance from the disc center and classically allowed regions for electronic states bound to the disk edge. r_t is the turning point.

$$\rho_t = \max \left[\tilde{b}, \frac{H^*}{H} \sqrt{1 - \left(E + \frac{q\tilde{b}H}{2H^*} \right)^2} \right]. \quad (7)$$

For the Meissner state of the disk ($m=0$) one finally obtains

$$F \left\{ \tilde{b}, \left(\frac{H^*}{H} \right)^2 \left[1 - \left(E + \frac{q\tilde{b}H}{2H^*} \right)^2 \right] \right\} = \frac{\pi \xi q H^* (n + \gamma)}{RH}, \quad (8)$$

$$F(\tilde{b}, x) = \sqrt{1 - \tilde{b}^2} \sqrt{1 - x} + (\tilde{b}^2 - x) \ln \frac{\sqrt{1 - \tilde{b}^2} + \sqrt{1 - x}}{\sqrt{|\tilde{b}^2 - x|}}.$$

For impact parameters \tilde{b} close to unity (i.e., for large angular momenta $\mu \sim k_r R$) and $k_r/k_F = q = 1$ each n th energy branch has a minimum as a function of two variables: impact parameter \tilde{b} and momentum k_r (see also Fig. 4 in Ref. 6). These two-dimensional local minima result in the appearance of a set of discontinuities (steplike structure) in the energy and magnetic field dependences of the density of states (DOS).

The above results for edge states can be easily extended to the case where a multiquanta vortex ($m \neq 0$) is located at the center of the sample. To this end one merely has to replace the magnetic field H by the expression $H - mH^* \xi/R$. This simple recipe works only for low-energy levels corresponding to the classically allowed regions near the disk edge [$\rho_t > \sqrt{m \xi H^* / (RH)}$]. By increasing the magnetic field one induces transitions between the states with different numbers m and, as a consequence, switching between energy branches with different m occurs. Each fluxoid entering the disk reduces the depth of the edge potential well for QP excitations and thus shifts the localized levels to higher energies. Upon further increase of the magnetic field the screening current and therefore the depth of the potential well increase and bound states are pressed down. Then next vortex comes in the states jump up again, resulting thus in oscillations of the DOS with the period $\delta H \sim \phi_0 / R^2$. The amplitude of such oscillations grows as in the size R decreases; therefore such oscillations are observable only in mesoscopic samples with the sufficiently small radii.

C. Multiquanta flux structures

Now we turn to the QP states which are bound to vortices penetrating the sample. To start with we consider the most simple case when all the vortices merge into a single giant vortex with a winding number m . $m=1$ corresponds to a conventional singly quantized vortex. According to general theory,¹¹ the number of anomalous energy branches (per spin) crossing the Fermi level should be equal to m . For a vortex carrying an odd number of the flux quanta one of this energy branches crosses Fermi level at zero impact parameter and, thus, is responsible for the peak in the DOS at the vortex center. On the contrary, for a vortex with an even number m there is no such an energy branch and no peak at the vortex center. All anomalous branches in this case cross the Fermi level at finite impact parameters $\mu \sim k_F r_c$, where r_c is the core radius. Generally the spatial distribution of the DOS has the shape of rings with radii of the order of ξ . The number of rings is determined by the winding number. Recently such solutions have been studied numerically in a number of works.¹²⁻¹⁴ An analytical approach for the description of QP states in multiquanta vortices can be developed using the quasiclassical method. Following the procedure described, e.g., in Ref. 15 one can consider a model with a step pair potential and obtain the QP energy vs the dimensionless impact parameter $\beta = \mu/(k_F \xi) = \tilde{b}R/\xi$:

$$E_{nm} = \frac{1}{1 + 2x_c/q} \left(\frac{\pi}{2} - \pi n + m \arctan \frac{x_c}{\beta} + \int_{x_c}^{\infty} \frac{m \beta e^{2(x_c-x)/q}}{x^2 + \beta^2} dx \right), \quad (9)$$

$x_c = \sqrt{\beta_c^2 - \beta^2}$, $\beta_c = r_c/\xi$, and n is an integer.

For low energies $\varepsilon \ll \Delta_0 (E \ll 1)$ we can linearize the energy spectrum for each anomalous branch: $E_{nm}(\beta) \approx a_{nm}(\beta_{nm} - \beta)$, where the coefficient

$$a_{nm} = \frac{m}{\beta_c \sqrt{1 - (\beta_{nm}/\beta_c)^2} [1 + 2(\beta_c/q) \sqrt{1 - (\beta_{nm}/\beta_c)^2}]}$$

is of the order unity, and an approximate expression for β_{nm} reads¹⁴

$$\beta_{nm}^* \approx \pm \beta_c \cos \frac{\pi(1-2n)}{2m}, \quad \frac{1-m}{2} < n < \frac{1+m}{2}.$$

Each energy branch crossing zero energy at a nonzero impact parameter is characterized by a certain number n (for the branch with $\beta_{nm} = 0$ the n number changes with a change of the impact parameter sign). Making use of the quasiclassical approach we also can find the corresponding spatial distribution of the density of states (DOS). Convolving the DOS with the thermal broadening function we obtain the quantity which is directly related to the local zero-bias tunneling conductance for transport between two reservoirs and, thus, can be probed by scanning tunneling spectroscopy measurements.¹⁶ In the clean limit the expression for this finite temperature tunneling conductance reads

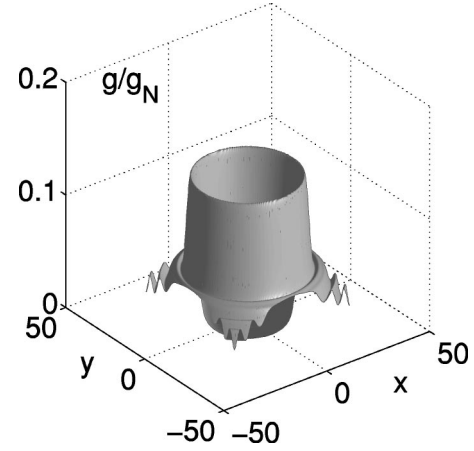


FIG. 2. Local zero bias tunneling conductance $g(\mathbf{r})/g_N$ for a multiquanta vortex with $m=2$; x, y coordinates are measured in $1/k_F$, $T \sim \Delta/(k_F \xi)$, $k_F r_c = 20\sqrt{2}$.

$$g(\mathbf{r}) = g_N \int_{-\infty}^{+\infty} \frac{N(\varepsilon, \mathbf{r}) d\varepsilon}{4N_F T \cosh^2(\varepsilon/2T)}, \quad (10)$$

where g_N is the normal state conductance and $N(\varepsilon, \mathbf{r})$ is the QP density of states. Shown on Figs. 2 and 3 is a normalized tunneling conductance $g(\mathbf{r})/g_N$ corresponding to $m=2, 3$ which generally, has a shape of rings with radii of the order of ξ [$T \sim \Delta_0/(k_F \xi)$; $k_F r_c = 20\sqrt{2}$ for $m=2$ and $k_F r_c = 40/\sqrt{3}$ for $m=3$]. The number of rings is determined by the winding number.

D. Vortex molecules

Now we derive quasiparticle DOS in the vortex molecule state. In macroscopic samples the structures consisting of several vortices with $a < \xi$ or multiquanta vortex solutions are energetically unfavorable due to the strong repulsion forces between the singly quantized vortices. On the contrary, in mesoscopic samples such structures appear stable even for $H \ll H_{c2}$, since Meissner currents push few vortices

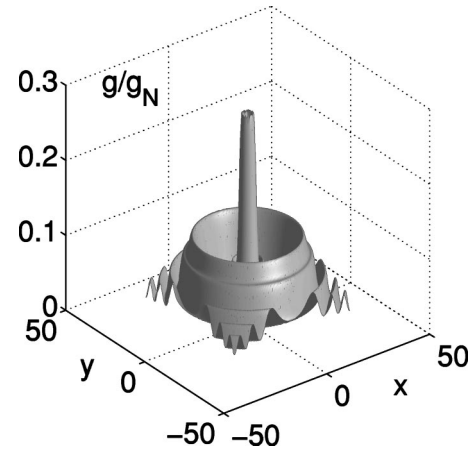


FIG. 3. Local zero bias tunneling conductance $g(\mathbf{r})/g_N$ for a multiquanta vortex with $m=3$; x, y coordinates are measured in $1/k_F$, $T \sim \Delta/(k_F \xi)$, $k_F r_c = 40/\sqrt{3}$.

present in the sample close together. Then the electronic states in a vortex molecule with $a \leq \xi$ differ strongly from the ones for isolated vortices due to the essential interference effects. The quantum-mechanical motion of low-energy quasiparticles is determined by the geometry of the vortex molecule involved. In small molecules splitting can be treated as a perturbation.

For a finite size of a vortex molecule ($D \neq 0$) the harmonics characterized by different μ interact and the angular momentum is no more a good quantum number. Nevertheless for small molecules the wave functions can be obtained using the perturbation theory which allows us to clarify the main qualitative features in the behavior of the local DOS. In the first order of this perturbation theory the wave functions for a $m\phi_0$ -vortex molecule take the form

$$\hat{\phi}_\mu = \hat{\phi}_\mu^{(0)} + \alpha_- \hat{\phi}_{\mu-m}^{(0)} + \alpha_+ \hat{\phi}_{\mu+m}^{(0)}, \quad (11)$$

$$\alpha_- = \frac{1}{E_\mu - E_{\mu-m}} \int_0^\infty u_{\mu-m} v_\mu D(r) r dr, \quad (12)$$

$$\alpha_+ = \frac{1}{E_\mu - E_{\mu+m}} \int_0^\infty u_\mu v_{\mu+m} D(r) r dr, \quad (13)$$

where $(u_\mu, v_\mu) = \hat{f}_\mu^{(0)}$ is the wave function for a giant m -quanta vortex. A qualitative (and most simple) picture can be obtained if we consider the asymptotical behavior of wave functions and DOS in the small distance limit $r < r_c$ and neglect the Andreev reflection inside this domain (put the gap $\Delta = 0$ in BdG equations, i.e., consider a model with a step pair potential¹⁵). The zero order terms in QP wave functions take the form

$$\hat{f}_\mu^{(0)} \simeq A \begin{pmatrix} e^{i\gamma_\mu} J_{|\mu+m/2|}(k_r r) \\ J_{|\mu-m/2|}(k_r r) \end{pmatrix}, \quad (14)$$

where the constant $A \sim \sqrt{k_r/r_c}$ is determined from normalization condition and the phase $\gamma_\mu = \pi n$ depends on the energy branch number and is determined from the matching with a large distance solution. The above approximation allows us to estimate the coefficients α_\pm for a certain branch characterized by a number n :

$$\alpha_+ \simeq \frac{k_r \xi e^{i\gamma_\mu} r_d^2}{m a_{nm} r_c^2} \left(\frac{a}{r_c}\right)^m \int_0^\infty J_{|\mu+m/2|}^2(k_r r_d x) e^{-x^2} x dx \quad (15)$$

[we have assumed here $D = (a/\xi)^m \exp(-r^2/r_d^2)$]. Evaluating the integrals one obtains

$$\alpha_+ \simeq \frac{k_r \xi r_d^2 e^{i\gamma_\mu}}{2 m a_{nm} r_c^2} \left(\frac{a}{r_c}\right)^m I_{|\mu+m/2|} \left(\frac{(k_r r_d)^2}{2}\right) e^{-(k_r r_d)^2/2}, \quad (16)$$

where I_μ is the modified Bessel function. Using the asymptotical expressions for these functions we get the final estimate

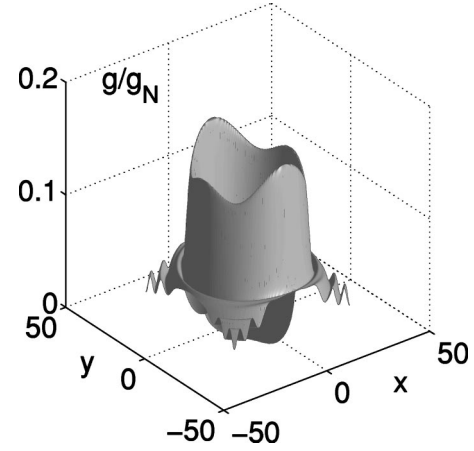


FIG. 4. Local zero bias tunneling conductance for a vortex molecule with $m=2$; x, y coordinates are measured in $1/k_F$, $T \sim \Delta/(k_F \xi)$, $k_F r_c = 20\sqrt{2}$.

$$\alpha_+ \simeq \frac{r_d \xi e^{i\gamma_\mu}}{2 \sqrt{\pi} m a_{nm} r_c^2} \left(\frac{a}{r_c}\right)^m, \quad \alpha_- = -\alpha_+ \exp(i\gamma_{\mu-m} - i\gamma_\mu). \quad (17)$$

To simplify calculations one can take a cylindrical Fermi surface without much loss in generality, so that k_z dependence may be neglected, $k_r = k_F$ (such a choice is well justified for NbSe₂), and finally arrive at the local DOS for a vortex molecule:

$$N(\varepsilon, \mathbf{r}) = A^2 \sum_\mu \delta(\varepsilon - \varepsilon_{nm}) \{ J_{|\mu+m/2|}^2(k_F r) + t_{nm} J_{|\mu+m/2|}(k_F r) [J_{|\mu+3m/2|}(k_F r) \cos(m\theta) + \gamma_{\mu+m}] - J_{|\mu-m/2|}(k_F r) \cos(m\theta + \gamma_\mu) \}, \quad (18)$$

where $t_{nm} = 2|\alpha_+|$.

One can observe that as soon as the constituent single-quanta vortices in a giant m vortex start to separate, each ring of the maximal DOS around a giant fluxoid splits into m peaks. With an increase in the size a of the molecule and, accordingly, in vortex spacing, several of the DOS peaks merge and finally only m peaks at the centers of individual vortices survive. The specific peak structure in the DOS distribution around a small-size vortex molecule is a direct consequence of quantum-mechanical interference of Andreev states. As a next natural step we calculate the zero-bias tunneling conductance in the clean limit taking into account the finite temperature effect. Typical spatial distributions of the tunneling conductance for two particular cases of $2\phi_0$ - and $3\phi_0$ -vortex molecules ($m=2$ and $m=3$) are shown in Figs. 4 and 5. Here we choose the following parameters: $t_{nm} = 0.7, T \sim \Delta_0/(k_F \xi), k_F r_c = 20\sqrt{2}$ for $m=2$, and $k_F r_c = 40/\sqrt{3}$ for $m=3$. The multipeak structure inside the core of a small-size molecule is surely smeared due to the finite lifetime and temperature effects. Thus, we can conclude that the

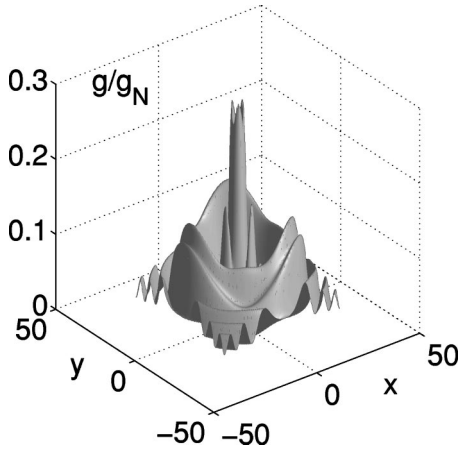


FIG. 5. Local zero bias tunneling conductance for a vortex molecule with $m=3$; x, y coordinates are measured in $1/k_F$, $T \sim \Delta/(k_F\xi)$, $k_F r_c = 40/\sqrt{3}$.

nontrivial behavior of the local DOS discussed above might become observable in the cleanest mesoscopic samples at low temperatures.

II. BALLISTIC TRANSPORT ALONG VORTEX LINES IN MESOSCOPIC SUPERCONDUCTORS: FLUX SENSITIVE ANDREEV WAVEGUIDES

In this section we turn to the description of phase-coherent transport properties of a few fluxoid superconductor (FFS). Consider mesoscopic superconducting disc squeezed between the leads connected to two normal reservoirs [see also Fig. 1(a) in Ref. 6]. Hereafter we assume the dimensions of a few-fluxoid sample to be much less than the phase-breaking length (characterizing the distance at which the phase coherence of the quantum-mechanical state is lost and determined by the rate of inelastic scattering). This assumption seems to be reasonable since the typical dimensions of few-fluxoid samples used in recent experiments² are of the order of several coherence lengths $\xi \sim \hbar V_F/\Delta$ (V_F is the Fermi velocity). For simplicity we also neglect the impurity scattering and, thus, restrict ourselves to the ballistic limit. The idea now is that in the sufficiently thin discs and low temperatures the ballistic transport will be carried by quasiparticles tunneling through the sample. Then every additional flux quantum entering the disc to form the vortex molecule or the multiquanta giant vortex will open an additional transport channel giving rise thus to a steplike increase in the disc conductance. The quantum-mechanical motion of low-energy quasiparticles (and hence the transmission coefficient) is determined by the geometry of a vortex molecule as well as by the geometry of a mesoscopic sample. Now we quantify this idea and develop a theory of the vortex mediated ballistic transport in FFS's.

In the homogeneous superconducting disc (without vortices) of the thickness larger than the coherence length the zero bias conductance for each normal-metal–superconductor boundary at $T=0$ is provided only by two-particle Andreev processes (single-particle tunneling is sup-

pressed because of the superconducting gap). The contribution of these processes to the conductance is proportional to T^2 , where T is a probability of transmission through the barrier separating the normal lead and the superconducting sample.

Within the most simple phenomenological approach the influence of vortices entering the sample on the transport characteristics can be described if we view a vortex core as a normal tube with the DOS coinciding with that in the normal metal.¹⁷ A more profound theoretical description of the effect of trapped vortices on the properties of Josephson tunnel junctions is based on the analysis of the modification of the Green's functions of superconducting electrodes in the core region.¹⁸ If we choose to apply this model for the estimate of conductance along the vortex line we immediately obtain the value proportional to the standard Sharvin's conductance

$$G_N \propto T \frac{e^2 k_F^2 \xi^2}{\hbar}.$$

The above estimate can be correct only for finite temperatures $T > \Delta/(k_F\xi)$ since the QP spectrum in the core of a singly quantized vortex is gapped. Using this estimate we assume that the conductance is determined by the density of states integrated over the vortex core and convolved with the thermal broadening function. Thus, such a consideration is based, in fact, on a transfer Hamiltonian approach and its validity is known to depend on the nature of the barrier region. This approach is obviously correct for incoherent tunneling into vortex states (the part of electron momentum parallel to the barrier plane is not conserved). In the case of coherent tunneling the above arguments should be regarded with caution. In this case the in-plane momentum (perpendicular to the vortex axis) should be conserved and, thus, is determined by its values allowed within the core. For incoming particles with a certain energy $\varepsilon \ll \Delta$ the allowed in-plane momenta for the states propagating along the core are given by the expression $k_r \approx \mu\Delta/(\varepsilon\xi)$. This restriction on the quantum numbers of transverse modes results in a strong suppression of vortex conductance. A simple estimate can be suggested in the spirit of Landauer approach if we just sum up the contributions of different transverse modes assuming equal transparencies for all modes ($\propto T$):

$$G \sim \frac{e^2}{\hbar} T \sum_{\mu} f[\varepsilon_{\mu}(k_z=0)], \quad (19)$$

where f is the Fermi distribution function. In the limit $\Delta/(k_F\xi) \ll T \ll \Delta$ we can replace the sum over μ by the integral and finally obtain the following estimate for this intermediate-temperature region:

$$G \sim \frac{e^2}{\hbar} T k_F \xi \frac{T}{\Delta}.$$

Such a suppression of conductance is directly related to the fact that the Caroli–de Gennes–Matricon energy levels are determined only by two quantum number: μ and k_z . A set of levels corresponding to the change in the third quantum number (which is, in fact, the radial part of momentum) is shifted to higher energies ($\varepsilon \sim \Delta$). This effective reduction

of the system dimensionality results in the fact that conductance is proportional to the core radius and not to its area.

All the above consideration is based on the assumption that the only contribution to the vortex conductance comes from the resonant temperature-activated transport through the Caroli–de Gennes–Matricon energy states, which can propagate along the flux line. However, even for zero temperature the single particle transport along the vortex line is possible due to the tunneling of electrons through the sample of a finite thickness L . Provided the energy of an incoming electron does not coincide with the Caroli–de Gennes–Matricon levels QP states decay into the sample due to multiple Andreev reflections from the boundaries of the vortex core over a certain characteristic distance L_d . The channels which satisfy the condition $L_d > L$ (these channels are open for single particle tunneling) will contribute the conductance of the mesoscopic system. The length L_d is a characteristic scale for conversion of normal current of incoming electrons into the superflow. In a macroscopic superconducting system the core states do not contribute to the electroconductivity along the vortex lines since the normal current injected into the sample converts to supercurrent at a length scale which is less than the sample size L . In other words, in this case the quasiparticle channels are shunted by the condensate.

Thus, in order to find FFS conductance in a finite length sample we have to describe the decay of the Andreev states along the vortex line. We are interested in the states at zero energy which can not propagate along the line because of the finite minigap in the core. Let us start from the BdG equations (4) for a single vortex line, which are written for radial parts of electronlike and holelike wave functions. Note that we assume here the k_z momentum to be complex valued to describe the electronic states with arbitrary energies ε . It is obvious that if the energy coincides with a certain discrete CdGM level the k_z momentum will be real and we must obtain the standard electronic states propagating along the vortex waveguide. Otherwise the imaginary part of the k_z momentum will give us the inverse decay length for electronic wave functions.

A. Propagation of quasiparticles along a normal metal cylinder in a superconductor in the absence of supercurrents ($V_s = 0$)

We start from the consideration of the case $V_s = 0$ and analyze the possibility to obtain the states localized in the xy plane (and decaying in the z direction) because of the well in the gap potential $\Delta(r)$. Provided the gap is zero within the domain $r < a$, this situation corresponds to the states in a normal metal cylinder of the radius a which is placed into a superconductor. Usual Andreev states with real k_z are gapped: if we take $a \sim \xi$ and $k_r \sim k_F$ the minimum energy is of the order of $\Delta(\infty)$. There are no states with real k_r for $\varepsilon = 0$.

For the particular case $\varepsilon = 0$ we can write the BdG equations (4) in the form of two decoupled equations if we take the wave functions in the form

$$\hat{f} = \Psi_+ \begin{pmatrix} 1 \\ i \end{pmatrix} + \Psi_- \begin{pmatrix} 1 \\ -i \end{pmatrix}. \quad (20)$$

The equations for the functions Ψ_+ and Ψ_- read

$$[\hat{h} \pm i\Delta(r)]\Psi_{\pm} = 0, \quad (21)$$

$$\hat{h} = \frac{\hbar^2}{2M} \left(-\frac{\partial^2}{\partial r^2} - \frac{1}{r} \frac{\partial}{\partial r} + \frac{\mu^2}{r^2} - k_r^2 \right). \quad (22)$$

The behavior of wave functions can be easily understood using the following simple analogy in standard electrodynamics. Equation (21) describes the propagation of waves in a waveguide with waveguide faces made of metal with finite conductivity which depends on r and, thus, complex dielectric constant takes the form

$$\varepsilon_d = 1 + \frac{i2k_F}{\xi k_r^2} \delta(r),$$

where $\delta(r) = \Delta(r)/\Delta(\infty)$. The skin depth in waveguide faces is proportional to the coherence length. Such an analogy allows one to conclude immediately that the waves with momentum close to the waveguide axis decay most slowly along this axis since the dissipation in waveguide faces in this case is minimal. We can also note that the waves with momenta direction far from the waveguide axis cannot propagate and decay at a length of the order of the waveguide radius.

Let us now discuss the solution of Eq. (21) in more detail. Within the standard quasiclassical approximation (assuming $k_r \xi \gg 1$) this solution can be written in the form (we take the equation for Ψ_+ for definiteness) $\Psi_+ = g_1(r)H_{\mu}^{(1)}(k_r r) + g_2(r)H_{\mu}^{(2)}(k_r r)$, where $H_{\mu}^{(1,2)}(k_r r)$ are Hankel functions and $g_{1,2}$ are slowly varying envelopes. Far from the normal metal cylinder ($r \gg a, \Delta = \text{const}$) we have the two exact solutions $H_{\mu}^{(1,2)}(r\sqrt{k_r^2 - 2ik_F/\xi})$. Inside the normal metal cylinder ($\Delta = 0$) there are also two exact solutions $H_{\mu}^{(1,2)}(k_r r)$. To avoid a divergence of the wave function for $r \rightarrow 0$ we must match the two independent solutions at the origin and obtain Bessel function for small r . One can see that for nonzero imaginary part of the wave vector $\sqrt{k_r^2 - 2ik_F/\xi}$ only one of Hankel functions [i.e., $H_{\mu}^{(2)}(r\sqrt{k_r^2 - 2ik_F/\xi})$] can exist at large distances since another Hankel function appears to diverge for $r \rightarrow \infty$. As a result, if we neglect small scattering (caused by the gap inhomogeneity) between the waves described by the envelopes $g_{1,2}$ (in quasiclassical approximation such scattering is zero) we cannot obtain the solution regular at the origin. The only way to get such a solution within the quasiclassical approximation is to put $\text{Im}(\sqrt{k_r^2 - 2ik_F/\xi}) = 0$ (which allows us to consider both Hankel functions at large distances), i.e., we must take $\text{Re}(k_r)\text{Im}(k_r) = k_F/\xi$, i.e., $\text{Im}(k_z) = k_F/[\xi \text{Re}(k_z)]$. The corresponding decay length along the z direction in this case appears to be the same as for the case of homogeneous su-

perconductor without normal-metal cylinder. Such modes are not localized in the (xy) plane—they are not waveguidelike solutions.

To get a waveguidelike solution we must go beyond the quasiclassical approximation and take account of the interaction of the waves described by the envelopes $g_{1,2}$. This scattering is indeed small (at least for $k_r \gg 1/\xi$) but it is this mechanism which allows us to obtain modes propagating in the waveguide. Such observation of the important role of nonquasiclassical corrections for the description of quasiparticles moving rapidly in the direction parallel to the normal-metal–superconductor interface is in agreement with the analysis^{19,20} of the bound states in SNS sandwiches. To obtain the solution we can consider a simple model with a step-like gap potential $\Delta=0$ for $r<a$ and $\Delta=\Delta_0$ for $r>a$. For $r>a$ we must consider only one of the Hankel function which decays with an increase in r : $\Psi_+ = T_+ H_\mu^{(2)}(r\sqrt{k_r^2 - 2ik_F/\xi})$. Inside the normal cylinder ($r < a$) the general solution can be taken in the form $\Psi_+ = H_\mu^{(2)}(k_r r) + R_+ H_\mu^{(1)}(k_r r)$. One can match the wave function and its first derivative at the NS boundary and obtain the reflection (R_+) and transmission (T_+) amplitudes. In the limit $k_r^2 \xi/k_F \gg 1$ (which is easy to get even for $k_r \ll k_F$) and $k_r a > \mu$ the reflection coefficient is

$$R_+ = R_0 \exp[-2ik_r a + i\pi(\mu + 1)], \quad (23)$$

where $R_0 \simeq k_F/[2(\text{Re } k_r)^2 \xi] \ll 1$ is the nonquasiclassical reflection coefficient from the NS boundary. Note that the same procedure can be made for Ψ_- : the reflection amplitude in this case takes the form

$$R_- = R_0 \exp[2ik_r a - i\pi(\mu + 1)]. \quad (24)$$

To obtain the solution regular at the origin we must put $R_\pm = 1$ (in this case the sum of Hankel functions inside the cylinder equals to the Bessel function). As a result, $\text{Re}(k_r)$ appears to be quantized: $\text{Re}(k_r) = \pi n/a + \pi(\mu + 1)/(2a)$, where n is an integer. The imaginary part of k_r also appears to be nonzero: $\text{Im}(k_r) = 0.5a^{-1} \ln \Lambda$, where we assume $\Lambda = R_0^{-1} \gg 1$. The corresponding expression for the imaginary part of k_z reads $\text{Im}(k_z) = \text{Re}(k_r)(\ln \Lambda)/[2\text{Re}(k_z)a]$. The above solution exist only for $\text{Im}(k_z) < k_F/[\xi \text{Re}(k_z)]$ [or in other words $\text{Im}(k_r) < k_F/(\text{Re } k_r \xi)$, i.e., $\text{Re}(k_r)/k_F < 2(\ln \Lambda)^{-1}a/\xi$]. The parameter $\Lambda^{-1} = R_0$ is the key parameter which controls the deviations from the quasiclassical model. In quasiclassical approximation we must take $\Lambda = \infty$ and the waveguidelike modes disappear.

If we do not take the steplike model for the gap (which overestimates the R_0 value) and consider a more realistic slowly changing gap profile (at a length scale of the order ξ), the reflection coefficient appears to be even smaller and Λ parameter is larger. Nevertheless the corresponding change in the decay length could be not so large because of the logarithmic dependence of this length on the Λ parameter.

B. Propagation of quasiparticles along the singly quantized vortex

The nonzero V_s is responsible for the interaction of the above waveguidelike solutions Ψ_+ and Ψ_- . To take account of such interaction we assume this mechanism to dominate only inside the core. As a result, we can treat the problem in several steps: (i) we calculate the nonquasiclassical reflection from the core boundary disregarding the V_s term near this boundary, (ii) we consider the core region following Refs. 5,15 to take account of the evolution of the relative phase between electronlike and holelike parts of the wave function caused by the Doppler shift. The first step gives us the expression for wave function near the core boundary, which can be used as a boundary condition for the solution inside the core:

$$\hat{f} = H_\mu^{(1)}(k_r r) \left[b \begin{pmatrix} e^{i\eta_1} \\ e^{-i\eta_1} \end{pmatrix} + a R_+ \begin{pmatrix} e^{-i\eta_2} \\ e^{i\eta_2} \end{pmatrix} \right] + H_\mu^{(2)}(k_r r) \left[a \begin{pmatrix} e^{-i\eta_3} \\ e^{i\eta_3} \end{pmatrix} + b R_- \begin{pmatrix} e^{i\eta_4} \\ e^{-i\eta_4} \end{pmatrix} \right]. \quad (25)$$

At the core boundary $\eta_1 = \eta_2 = \eta_3 = \eta_4 = \pi/4$. The final condition on the nonquasiclassical reflection coefficients after all matching procedures reads

$$\sin(\varepsilon_\mu/\Delta_0) \simeq \frac{R_+ + R_-}{1 + R_0^2}, \quad (26)$$

where ε_μ is the CdGM spectrum for a singly quantized vortex. If we consider rather small μ values ($\mu \ll k_r r_c$) and neglect the terms proportional to R_0^2 the expression (26) can be rewritten as follows:

$$R_+ + R_- = 2R_0 \cos[2k_r r_c - \pi(\mu + 1)] \simeq \varepsilon_\mu/\Delta_0. \quad (27)$$

The inverse decay length along the z axis is given by the expression

$$\text{Im } k_{zn} \simeq \frac{\text{Re } k_{rn}}{2\text{Re } k_{zn} r_c} \ln(\Lambda \varepsilon_\mu/\Delta_0), \quad (28)$$

where the $\Lambda = R_0^{-1}$ parameter should be determined from the nonquasiclassical reflection problem discussed in Sec. II A, $\text{Re } k_{rn} = \pi n/r_c + \pi(\mu + 1)/(2r_c)$ and the $\Lambda \varepsilon_\mu/\Delta_0$ value is assumed to be large. One can see that the appearance of the superfluid velocity results in an increase of the decay length because of the small minigap value. For quasiparticles with momenta almost parallel to the vortex axis the decay length appears to be much larger than the coherence length.

C. Propagation of quasiparticles along the multiqanta vortices

The above consideration can be generalized for the case of a multiqanta vortex with a certain winding number m . Using the analogous procedure one obtains Eq. (26), where ε_μ is a set of anomalous branches discussed in Sec. I. The inverse decay length is given by the expression

$$\text{Im } k_{zn} \simeq \frac{\text{Re } k_{rn}}{2\text{Re } k_{zn} r_c} \text{arccosh}[\Lambda \sin(\varepsilon_\mu / \Delta_0) / 2]. \quad (29)$$

The core radius is known to increase with an increase in the winding number m (see, e.g., Ref. 14). According to Eq. (29) this fact results in the increase of the QP decay length. It should also be noted that for multiquanta vortices a finite number of bound states with $L_d = \infty$ appear to exist even at $\varepsilon = 0$ (there is no minigap contrary to the case of singly quantized vortex). For each anomalous energy branch there exists such a zero energy bound state characterized by the momentum $k_r \sim \mu / r_c$.

D. Conductance of a singly quantized vortex: Large area contacts

Let us estimate the ballistic conductance of the vortex of a certain length L . We assume that the superconducting disk with the vortex is placed between two normal-metal reservoirs. Provided the transparency of the tunnel barriers (which separate superconductor and these reservoirs) is small enough, the contribution of two-particle Andreev processes is suppressed. Let us estimate only the conductance contribution associated with the channels open for single particle tunneling along the vortex line. Each mode decaying along the vortex provides the conductance contribution $\propto e^2 \exp[-2\text{Im}(k_z)L] / \hbar$. The total contribution from the single particle processes can be written as

$$G_0 \propto \frac{e^2}{\hbar} \mathcal{T} \sum_{\mu} \sum_n \exp(-2\text{Im}k_{zn}L), \quad (30)$$

where k_{zn} is determined from Eq. (28). The value $\text{Re } k_{rn}$ meets the condition $\text{Re } k_{rn} > \mu / r_c$ (otherwise the turning point μ / k_r of the Hankel function appears to be outside the core region). The maximum $\text{Re } k_{rn}$ value is determined by the Fermi wave vector ($\text{Re } k_{rn} < k_F$). As a result, we can put $\text{Re } k_{rn} = \pi n / r_c$, where $n_{\min} < n < n_{\max}$, $n_{\min} \sim \mu$, and $n_{\max} \sim k_F \xi$. We assume here that the transmission coefficient \mathcal{T} through the barrier is the same for all channels (in a more realistic model this coefficient surely depends on the quantum numbers). Taking $\xi < L < \xi^2 k_F$ one can see that the main contribution to the conductance G_0 is provided by the modes with momenta almost parallel to the vortex axis. As a result, we can put $\text{Re } k_z \simeq k_F$ in Eq. (28) and write the conductance in the form

$$G_0 \propto \frac{e^2}{\hbar} \mathcal{T} \sum_{\mu} \sum_{\mu}^{n_{\max}} \exp\left(-\frac{\pi n L \ln(\Lambda \mu / n)}{k_F r_c^2}\right). \quad (31)$$

Replacing the sums over μ and n by the integrals one obtains

$$G_0 \propto \frac{e^2}{\hbar} \mathcal{T} \int_0^{+\infty} d\mu \int_{\mu}^{n_{\max}} dn \exp\left(-\frac{\pi n L \ln(\Lambda \mu / n)}{k_F r_c^2}\right). \quad (32)$$

Neglecting the weak logarithmic dependence vs n in Eq. (32) we can evaluate the above integrals and obtain the final expression for the ballistic conductance

$$G_0 \propto \frac{e^2}{\hbar} \mathcal{T} (k_F \xi)^2 \frac{\xi^2}{L^2 (\ln \Lambda)^2}. \quad (33)$$

Comparing this expression with the Sharvin's conductance of the normal wire of the radius ξ , one can see that the decay of quasiparticle states along the vortex line results in a decrease of the Sharvin's conductance by the factor $\xi^2 / [L^2 (\ln \Lambda)^2]$. For mesoscopic samples with L of the order of several ξ this single particle contribution can be comparable with the two-particle Andreev contribution ($\propto \mathcal{T}^2$). For large L values ($L > k_F \xi^2$) the power law decay of the conductance vs L should be replaced by the exponential dependence $\sim \exp[-L \ln \Lambda / (k_F \xi^2)]$. Thus, in the large L limit the current through the single particle channels is shunted by the supercurrent.

E. Conductance of a multiquanta vortex: large area contacts

With an increase in magnetic field we change the winding number and hence a number of single particle channels. For large area contacts (with area larger than both the core radius and intervortex distance) all these vortex channels contribute to the conductance and, as a result, we obtain a stepwise conductance behavior vs magnetic field [see also Fig. 1(b) in Ref. 6]. For vortex structures consisting of m separated singly quantized vortices one can expect that the total conductance is given by the sum of isolated vortex contributions $G_{\Sigma}(m) = m G_0$. For giant vortices or vortex molecules the dependence of G_{Σ} vs m becomes more complicated and is mainly determined by the m dependence of the effective core radius $r_c(m)$:

$$G_{\Sigma} \propto \frac{e^2}{\hbar} \mathcal{T} [k_F r_c(m)]^2 \frac{r_c^2(m)}{L^2}. \quad (34)$$

Note that the zero energy states provide an additional contribution to conductance of the order of $(e^2 / \hbar) \mathcal{T} k_F r_c(m) 2[m/2]$, where square brackets denote an integer part.

F. Conductance of multiquanta vortices: Small area contacts

For point contacts with an area of the contact much smaller than the area of the giant vortex core r_c we should take account of the dependence of the transmission coefficient \mathcal{T} vs μ . As a result, the efficiency of single particle channels depends on the winding number m and point contact position.

At small distances from the giant vortex center the wave functions have Bessel asymptotics and, thus, vanish inside the domain $r < |\mu + m/2| / k_r$. As a result, for point contact positioned at the giant vortex center the transmission coefficient should also vanish for modes with $|\mu + m/2| > k_r d$, where $d \ll r_c$ is the contact radius. Thus, in this case we should take $n_{\min} \sim \max[\mu r_c / d, r_c / d]$ and the expression for the conductance reads

$$G_0 \propto \frac{e^2}{\hbar} T \sum_{\mu} \sum_{n_{\min}}^{n_{\max}} \exp\left(-\frac{\pi n L \ln(\Lambda_{\mu n})}{k_F r_c^2}\right), \quad (35)$$

where $\Lambda_{\mu n} = \Lambda \varepsilon_{\mu}(k_{rn})/\Delta_0$. For odd winding numbers the spectrum has a branch crossing Fermi level at $\mu=0$ [$\varepsilon_{\mu}(k_{rn})/\Delta_0 \sim \mu/(k_{rn} r_c) \sim \mu/n, \Lambda_{\mu n} \sim \Lambda \mu/n$]. For even winding numbers there is no such an energy branch and for small μ we should take $\varepsilon_{\mu}(k_{rn})/\Delta_0 \sim 1$ and $\Lambda_{\mu n} \sim \Lambda$. For rather small contact radius $d < L/(k_F r_c)$ the terms in the sum (35) vanish very fast with an increase in n and μ : the main contribution to the conductance comes from the first term with minimal n and μ . The conductance for odd and even winding numbers m takes the form

$$G_{\text{odd}} \propto \frac{e^2}{\hbar} T \exp\left(-\frac{L \ln(\Lambda d/r_c)}{k_F r_c d}\right),$$

$$G_{\text{even}} \propto \frac{e^2}{\hbar} T \exp\left(-\frac{L \ln \Lambda}{k_F r_c d}\right).$$

For the ratio of conductances we obtain

$$\frac{G_{\text{even}}}{G_{\text{odd}}} \sim \left(\frac{d}{r_c}\right)^{L/k_F r_c d} \ll 1.$$

The suppression of the conductance G_{even} is caused by the absence of the anomalous energy branch crossing Fermi level at $\mu=0$ for even winding numbers. Such an odd-even effect results in alternating behavior of conductance as a function of magnetic field [Fig. 1(b) in Ref. 6]. Generally the behavior of conductance vs magnetic field is determined by the interplay of steplike and oscillating contributions.

III. CONCLUSIONS

To summarize, we have developed a theory of quasiparticle excitations in the vortex state of mesoscopic superconductors. We have found spatial distribution of the QP density of states, investigated ballistic transport through the vortex

cores and analyzed the regimes of alternating and steplike behaviors of conductance. The steps on the dependence of conductance vs magnetic field are associated with the first-order phase transitions between the states with different winding numbers and, thus, should exhibit strong hysteresis. Note, that the oscillatory behavior on the STS characteristics (vs magnetic field) at the disk center as well as the suppression of the gap value at the disk edge by a magnetic field and hysteresis have been observed in recent experiments²¹ carried out on mesoscopic In disks. A similar behavior of the conductance is observed in so-called Andreev interferometers (see Ref. 22 for review) measuring the phase difference between two superconductors. Thus, the transport measurements of a superconducting disk with a few fluxoids provide a possibility to realize a new type of mesoscopic Andreev interferometers (or fluxometers). Another possibility to realize such Andreev fluxometer is to consider the electron transport through superconducting constrictions (of the minimum diameter of several coherence lengths) in a strong magnetic field which destroy the superconducting order parameter in the bulk. In such a strong field a superconducting nucleus with a few trapped vortices can still exist inside the constriction and result in quantum behavior of conductance vs magnetic field. A simple example of such a system is a superconducting STM tip. Alternatively a constriction can be fabricated by the technique²³ based on pressing a normal metal STM tip to a superconducting substrate.

ACKNOWLEDGMENTS

We thank G. Crabtree, Yu. Galperin, G. Karapetrov, A. Koshelev, N. Kopnin, V. Kozub, V. Moshchalkov, D.A. Ryzhov, S.V. Sharov, I.A. Shereshevsky, and I.D. Tokman for useful discussions. This work was supported by the U.S. DOE, Office of Science under Contract No. W-31-109-ENG-38, NATO Collaborative Linkage Grant No. PST.CLG.978122, Russian Foundation for Fundamental Research, Grant No. 00-02-16158, and by the Russian Academy of Sciences under the Program ‘‘Quantum Macrophysics.’’

¹G. Boato, G. Gallinaro, and C. Rizzuto, *Solid State Commun.* **3**, 173 (1965); D.S. McLachlan, *ibid.* **8**, 1589 (1970); **8**, 1595 (1970); D.S. McLachlan, *Phys. Rev. Lett.* **23**, 1434 (1969).

²A.K. Geim, S.V. Dubonos, J.J. Palacios, I.V. Grigorieva, M. Henini, and J.J. Schermer, *Phys. Rev. Lett.* **85**, 1528 (2000).

³V.A. Schweigert, F.M. Peeters, and P.S. Deo, *Phys. Rev. Lett.* **81**, 2783 (1998); J.J. Palacios, *Phys. Rev. B* **58**, R5948 (1998).

⁴Recent GL simulations, L.F. Chibotaru, A. Ceulemans, V. Bruynndoncx, and V. Moshchalkov, *Nature (London)* **408**, 833 (2000), revealed a fascinating effect of formation stable vortex-antivortex structures near H_{c2} . However, the conductivity effects we discuss occur at low fields $H \ll H_{c2}$, and therefore these particular vortex structures are not relevant for the consideration to follow. The authors are grateful to Professor V. Moshchalkov for pointing this out.

⁵C. Caroli, P.G. de Gennes, and J. Matricon, *Phys. Lett.* **9**, 307 (1964).

⁶A.S. Mel'nikov and V.M. Vinokur, *Nature (London)* **415**, 60 (2002).

⁷I. Giaever, in *Tunneling Phenomena in Solids*, edited by E. Burstein and S. Lundqvist (Plenum Press, New York, 1969), pp. 255–271.

⁸P. Pincus, *Phys. Rev. B* **158**, 346 (1967).

⁹M.Ya. Azbel and A.Ya. Blank, *Pis'ma Zh. Éksp. Teor. Fiz.* **10**, 49 (1969).

¹⁰P.W. Anderson, *J. Phys. Chem. Solids* **11**, 28 (1959); Jan von Delft, A.D. Zaikin, D.S. Golubev, and W. Tichi, *Phys. Rev. Lett.* **77**, 3189 (1996); K.A. Matveev and A.I. Larkin, *ibid.* **78**, 3749 (1997); F. Braun and Jan von Delft, *Phys. Rev. B* **59**, 9527 (1999).

¹¹G.E. Volovik, *Pis'ma Zh. Éksp. Teor. Fiz.* **57**, 233 (1993) [*JETP Lett.* **57**, 244 (1993)].

¹²D. Rainer, J.A. Sauls, and D. Waxman, *Phys. Rev. B* **54**, 10 094 (1996).

- ¹³Y. Tanaka, S. Kashiwaya, and H. Takayanagi, *Jpn. J. Appl. Phys.* **34**, 4566 (1995); Y. Tanaka, A. Hasegawa, and H. Takayanagi, *Solid State Commun.* **85**, 321 (1993).
- ¹⁴S.M.M. Virtanen and M.M. Salomaa, *Phys. Rev. B* **60**, 14 581 (1999).
- ¹⁵J. Bardeen, R. Kümmel, A.E. Jacobs, and L. Tewordt, *Phys. Rev.* **187**, 556 (1969).
- ¹⁶H.F. Hess, R.B. Robinson, R.C. Dynes, J.M. Valles, Jr., and J.V. Waszczak, *Phys. Rev. Lett.* **62**, 214 (1989); H.F. Hess, R.B. Robinson, and J.V. Waszczak, *ibid.* **64**, 2711 (1990); I. Maggio-Aprile, Ch. Renner, A. Erb, E. Walker, and O. Fisher, *ibid.* **75**, 2754 (1995); B.W. Hoogenboom, M. Kugler, B. Revaz, I. Maggio-Aprile, O. Fisher, and Ch. Renner, *Phys. Rev. B* **62**, 9179 (2000); S.H. Pan, E.W. Hudson, A.K. Gupta, K.-W. Ng, H. Eisaki, S. Uchida, and J.C. Davis, *Phys. Rev. Lett.* **85**, 1536 (2000).
- ¹⁷N. Uchida, K. Enpuku, Y. Matsugaki, S. Tomita, F. Irie, and K. Yoshida, *J. Appl. Phys.* **54**, 5287 (1983); N. Uchida, K. Enpuku, K. Yoshida, and F. Irie, *ibid.* **56**, 2558 (1984).
- ¹⁸A.A. Golubov and M.Yu. Kupriyanov, *J. Low Temp. Phys.* **70**, 83 (1988).
- ¹⁹O. Šipr and L. Györfy, *J. Phys.: Condens. Matter* **8**, 169 (1996).
- ²⁰R. Kümmel, *Phys. Rev. B* **10**, 2812 (1974).
- ²¹M. Zalalutdinov, H. Fujioka, Y. Hashimoto, S. Katsumoto, and Y. Iye, *Physica B* **284-288**, 817 (2000).
- ²²C.J. Lambert and R. Raimondi, *J. Phys.: Condens. Matter* **10**, 901 (1998).
- ²³M. Poza, E. Bascones, J.G. Rodrigo, N. Agrait, S. Vieira, and F. Guinea, *Phys. Rev. B* **58**, 11 173 (1998); H. Suderow, E. Bascones, W. Belzig, F. Guinea, and S. Vieira, *Europhys. Lett.* **50**, 749 (2000).